Published in final edited form as:

Ultrasound Med Biol. 2016 August ; 42(8): 1834–1847. doi:10.1016/j.ultrasmedbio.2016.02.020.

Towards deep brain monitoring with superficial EEG sensors plus neuromodulatory focused ultrasound

F Darvas, PhD[a], **E Mehić, MS**[a], **CJ Caler**[b], **JG Ojemann, MD**[a], and **PD Mourad, PhD**[a,b,c]

[a]Department of Neurosurgery, University of Washington, 1959 NE Pacific St, Seattle, WA 98105

[b]Department of Bioengineering, University of Washington, 3720 15th Ave NE, Seattle, WA 98105

[c]Division of Engineering and Mathematics, University of Washington, 18115 Campus Way NE, Bothell, WA 98011

Abstract

Noninvasive recordings of electrophysiological activity have limited anatomical specificity and depth. We hypothesized that spatially tagging a small volume of brain with a unique electroencephalogram (EEG) signal induced by pulsed focused ultrasound (pFU) could overcome those limitations. As a first step towards testing this hypothesis, we applied transcranial ultrasound (2 MHz, 200 microsecond-long pulses applied at 1050 Hz for one second at a spatial peak temporal average intensity of 1.4 W/cm^2) to the brains of anesthetized rats while simultaneously recording EEG signals. We observed a significant 1050 Hz electrophysiological signal only when ultrasound was applied to living brain. Moreover, amplitude demodulation of the EEG signal at 1050 Hz yielded measurement of gamma band (>30 Hz) brain activity consistent with direct measurements of that activity. These results represent preliminary support for use of pFU as a spatial tagging mechanism for non-invasive EEG-based mapping of deep brain activity with high spatial resolution.

Keywords

focused ultrasound; EEG; brain activity

INTRODUCTION

Management of neurological injuries and disorders, such as traumatic brain injury, epilepsy, depression, as well as control of neuroprosthetic devices, can require monitoring of the brain's electrical activity. Electroencephalography (EEG) exemplifies such monitoring, as it facilitates tracking of different stages of convulsive status epilepticus, important for early treatment (Maganti and Rutecki 2013). Here, we offer first steps towards a means of monitoring focal and deep brain activity through a combination of EEG and transcranially delivered pulsed focused ultrasound (pFU). This combination would permit extra-cranial monitoring of focal brain function, avoiding invasive procedures such as electrocorticography (ECoG).

Corresponding Author – Pierre D. Mourad (doumitt@uw.edu).

Current EEG techniques based on external electrodes can collect electrophysiological data at frequencies up to 1kHz (Fedele et al. 2015; Telenczuk et al. 2011; Teleńczuk et al. 2014)), with the bulk of measured endogenous activity occurring below 100 Hz (Darvas et al. 2010; Darvas et al. 2013; Smith et al. 2014; Dalal et al. 2008; Cheyne et al. 2008; Ball et al. 2008). However, extra-cranial electrodes can measure focal EEG signals for only superficial brain structures, with variable resolution and localization accuracy (Darvas et al. 2004). This leaves deep brain function inaccessible to external monitoring (Maganti and Rutecki 2013; Wennberg and Cheyne 2014). Barriers include signal non-uniqueness (superficial electrophysiological signals can arrive simultaneously with signals from deep brain), noise induced by motion artifacts, and the intrinsically weak nature of deep brain signals. The alternative, ECoG, an intra-cranially placed electrophysiological monitoring system, solves this problem but at obvious cost.

Ultrasound has been used to temporarily and non-destructively activate or inhibit central neural circuits. Using a cat model, the Fry brothers (e.g., Fry, 1958) demonstrated that unfocused 1MHz ultrasound reversibly and repeatably suppressed electrophysiologically-measured brain activity. This result is consistent with a contemporary and more exhaustive study (Ballentine et al., 1960), as well as the work of Vykhodtseya and Koroleva (1986) who generated cortical spreading depression in rat brain using ultrasound. Recently, Tyler and colleagues (Tyler et al., 2008; Tufail et al., 2010, 2011) demonstrated that pulsed, low intensity and low-frequency (0.5 MHz) unfocused ultrasound could activate neural circuits in mouse brain, through several means: direct measurement of action potentials within brain slice preparations, in intact brain, and direct observation of peripheral motor function. King et al. (2013, 2014) and Younan et al. (2013) produced comparable observations through a greater range of ultrasound frequencies. Yoo et al (2011) observed that transcranial pFU (at 0.69 MHz) could create functional changes in rabbit brain, including excitatory effects when applied to motor cortex, measurable with fMRI.

More recently, we (Mehić et al, 2014) used a high-frequency (2 MHz) system capable of focused delivery of very low-frequency ultrasound (‘modulated focused ultrasound [mFU]), as well as pFU, to demonstrate spatial variability of transcranial activation of brain circuits in mice on length scales of one millimeter, observed through induction of repeatable peripheral motor function. Also Deffieux et al. (2013) demonstrated reversible changes in macaque visual function after application of pFU at 0.32 MHz to their prefrontal cortex. Finally, Legon et al. (2014) showed modulation of the function of human primary somatosensory cortex with transcranial pFU delivered at 0.5 MHz, with further analysis of the associated EEG signals reported in Mueller et al. (2014) and discussed below. Lee et al. (2015) found results similar to that of Legon et al.

Of note, none of these studies report adverse events, determined through assay of histological or electrophysiological changes of brain or changes in grossly observed behavior. This is true despite the fact that several of these studies (e.g., King et al; Mehic et al; Trufall et al; Yoo et al) used, among several protocols, ultrasound with a spatial peak and temporal average intensity value greater than that given by FDA guidelines for diagnostic ultrasound, and then applied that ultrasound multiple times to the same location of brain (e.g., Yoo et al). This is likely due to the fact that while some of these protocols embody

ultrasound above those FDA guidelines for intensity, those protocols fall well below that used without acoustic contrast agents to create blood-brain barrier disruption (e.g., ~ 80 W/cm^2 spatial and temporal average intensity applied for 0.2 seconds, as found by Mesiwala et al, 2002).

All of the studies cited above that used EEG did so in order to measure brain activity generally at less than 50 Hz induced by application of ultrasound to the brain. In contrast to the present work, no studies to our knowledge have reported measurements of brain activity at the high frequencies associated with ultrasound application, here at the 1050 Hz pulsed repetition frequency of our ultrasound, let alone sought to extract low-frequency brain activity from those signals. Such analysis is of interest here because we seek, long term, to facilitate use of external EEG to monitor deep, focal brain function by 'tagging' that activity with a unique, detectable, high frequency electrical signal generated by application of pFU to the brain volume of interest. Here we describe completion of a first step towards this goal: successful demonstration that transcranially delivered pFU could generate from within rat brain a unique, high-frequency EEG signal measured extra-cranially, whose analysis yields measures of low-frequency brain activity consistent with their direct, extra-cranial measurement.

Materials and Methods

Methods –Tissue phantom and EEG Implantation

Here we sought to test the interaction between our ultrasound delivery system and the EEG electrodes *in vitro*, before *in viv*o studies. The medium used consisted of saline-based 4% alginate gel with mechanical properties (density and ultrasound attenuation) similar to rat brain while also being comparably conductive. We inserted 8 steel needle tip thin wire EEG electrodes (Ambu Neuroline Subdermal 27G, Cadwell, Kennewick, WA) into the gel in the same positioning and pattern by which we would insert them in a rat head (Figure 1) with approximately 3–4 mm between electrodes in the rostral/caudal direction, each line approximately 4 mm from midline. We also placed reference and ground electrodes. After electrode insertion, five locations were chosen for application of ultrasound: both outside, and within the two rows of electrodes, as well as beside, or directly above the electrodes. Using this *in vitro* experimental setup, we mirrored our *in vivo* ultrasound trial protocol with 50, instead of 100 trials, consistent with the low variance of our results. We also performed a test in which we decoupled the transducer from the alginate gel, in order to only allow any electromagnetic fields associated with the transducer to affect the electrode montage.

Methods – in vivo

All animal procedures were approved by the University of Washington Institutional Animal Care and Use Committee (IACUC), IACUC protocol number 4084-06.

Overview—We worked with four Sprague Dawley rats, weighing approximately 270g and aged 8 weeks. Isoflurane anesthesia was used at a 5% induction rate and then kept at 2%, with two liters/min oxygen flow at 100%. Toe and tail pinches were administered to insure adequate depth of anesthesia. After recording baseline brain activity without application of

ultrasound, we then apply ultrasound to the brain while recording brain activity. Next, we injected the animals with a lethal overdose of a combination of pentobarbital sodium and phenytoin sodium (Beuthanasia®-D, Merck Animal Health, Madison, NJ) while continuing the application of ultrasound and measurement of brain activity. This allowed use of the same setup to test for differences in the effect of pFU on live brain activity vs. inactive brain. Data was recorded post-injection for several minutes until death of the animal was confirmed by observation of a cessation of breathing and heartbeat, discoloration of the extremities, and nascent stiffening of the limbs.

EEG Implantation - in vivo

Under anesthesia, we implanted 8 thin-wire EEG electrodes into the rats' heads, as well as 1 reference electrode and 1 ground wire, as in our alginate setup (Figure 1). We first measured endogenous brain activity without ultrasound application, for approximately five minutes. For the next 200 seconds we then applied our transcranial ultrasound protocol, discussed below, centered 5 mm below the surface of the skin and into the left hemisphere of the brain, two mm away from the closest electrodes. We then compared brain activity during pFU application to living (anesthetized) brain versus the brain of an euthanized animal. To do so, we administered the rat an overdose (200mg/kg) of pentobarbital via intraperitoneal injection, which took approximately thirty seconds. After this injection we continued to record EEG, while applying ultrasound, until the animal expired, as measured by physiological signs.

Pulsed focused ultrasound (pFU) source

To implement the pFU protocol we used the ultrasound source and supporting electronics described in Mehić et al (2014) – also see our Figure 1 – a dual element, coaxial, confocal and circular transducer, and associated matching networks (H-148, Sonic Concepts, Woodinville, WA, U.S.) with a central opening filled with a passive cavitation hydrophone from Sonic Concepts. Two Agilent Series 33220A 20 MHz function generators (Agilent Technologies, Santa Clara, CA, U.S.), controlled by a third Agilent function generator drove two ENI brand model A150 55dB amplifiers (Electronic Navigation Industries, Rochester, NY, U.S.) that in turn powered each of the two elements within the focused transducer. We monitored the voltage entering each transducer element with a LeCroy Oscilloscope (Waverunner LT344, Teledyne LeCroy, Chestnut Ridge, NY, U.S.). We tuned each element of the focused transducer to emit ultrasound at 2 MHz, which together produced a spatial peak temporal average (SPTA) intensity of 8 W/cm^2– see calibration section below. The length and width of the focus of the transducer, measured at the full width half maximum value is 7 mm in the axial direction and 1.5 mm (diameter) in the lateral direction, with an associated volume of approximately 12.4 microliters. Figure 1 shows a schematic of this focal volume projected onto a rat brain.

Ultrasound Calibration

We calibrated our transducers using a calibrated needle hydrophone (HNR-1000, Onda Corporation, Sunnyvale, CA, U.S.) placed in a tank filled with degassed and deionized water. We put its active tip at the focus of each of the two elements of the dual-element transducer, and at the point of its maximum pressure. To ensure that the voltage into each

element of the dual-element transducer produced the same pressure (thereby equalizing the pressure at the focus from each element of the transducer), we measured the peak positive pressure with each element running individually, such that when used together, each of the two elements contributed half the total peak pressure at the focus.

Ultrasound Protocol

Ultrasound with a 2.0 MHz carrier frequency was delivered in pulses lasting 200 μs at a pulse repetition frequency of 1050 Hz. Its spatial peak temporal average intensity (I_spta) measured 11.9 W/cm^2 in degassed water with a calibrated hydrophone (HNR-0500, Onda Inc, Sunnyvale CA) and 1.4 W/cm^2 in degassed water after transmission through the top of a rat head (skin, fascia, skull). The pulse train was delivered for 1 second, followed by a 1 second rest period with no ultrasound. This process lasted 200 seconds (100 trials) before animals were injected with Beuthanasia and continued for 5 to 10 minutes after injection (Figure 2).

We note that we have tested the safety of the original protocol from Mehić et al during its pilot studies, in a preliminary way. For those pilot studies we applied ultrasound with the same carrier frequency as here, with a range of intensities (0.2–20 W/cm^2 I_spta, in water and without transmission through a skull), a pulse duration ranging between 100–300 μs, but at a larger pulse repetition frequency (1500 Hz versus 1050 Hz, hence nearly 50% more pulses). We did so in four rats in experiments lasting from one to three hours, with some breaks of a few minutes between studies as we contemplated the results. This contrasts with the present study, where we applied ultrasound for intervals of one second on and one second off, for a total of 200 seconds while the animal was alive, and another several minutes while the animal expired. Histological studies of the brains of rats collected during the pilot study showed no damage. This is consistent with the discussion on the safety of neuromodulatory ultrasound as thus far explored.

Delivery of Ultrasound

As described in Mehić et al. (2014) the top of the transducer was screwed to a plastic black ring attached to a metal arm. The concave side of the transducer (where ultrasound is emitted) was fitted with a hollow plastic cone, with a large opening covered by an approximately 100 micron-thick latex. The transducer housing was filled with degassed and deionized water, then attached to a metal arm connected to a micro positioner. The metal stage acts as a 3D–coordinate grid, where the micro positioner can move the transducer housing through the x–y, x–z, and y–z planes in sub-millimeter increments.

EEG recording

EEG was recorded from 8 sub-dermal needle electrodes (see montage in Figure 1) at a 4800 Hz sampling rate (rat #1) and then at 38,400 Hz (rats #2–4 and the alginate study) with a single 16-channel biosignal amplifier (gUSBamp, Guger Technologies, Graz, Austria) in a monopolar configuration. We increased the sampling rate after rat #1 to attempt to resolve higher frequencies in the EEG signal, but did not utilize the higher sampling rate data for this work. Data for rats #2–4 was thus subsequently down sampled by a factor of eight to 4800 Hz, using the MATLAB *RESAMPLE* function. Electrode impedance for each channel

was recorded before and after the experiment, and found to be less than 20 kohm across channels and experiments, except for the first animal, where four channels lost contact during recording and had to be discarded. All signals were recorded in continuous DC mode for the duration of each ultrasound stimulation experiment.

Onset of the pFU stimulation sequence was recorded with a digital trigger channel on the EEG amplifier which is sampled at the same rate as the analog input channels. The digital trigger was set high by the function generator controlling the pFU amplifier every time the pFU stimulation turned on.

EEG signal analysis - basic EEG preprocessing

In order to reduce contamination by artifacts common across all channels for a given rat, we applied a common average re-referencing (CAR) across all recorded channels by subtracting the mean across all channels from each channel individually. After filtering the data – details below - each data set was then segmented into trials based on the pFU onset trigger. Trials were either created in an interval of 1 second prior to stimulation onset to one second post stimulation onset, or 0.5 seconds prior to stimulation onset to 1.5 seconds post stimulation onset. The latter segmentation was used to show pFU off-on-off transitions. Post recording, one channel was removed from the alginate experiment due to lost contact, while we retained data from all channels for our *in* vivo studies. We removed individual trials with excessive (>50 uV) voltage spikes for each rat, from ten to 21 trials out of 100 for a given channel within a given study, depending on the rat, which is common practice for EEG signal analysis (Gevins et al., 1977). We then used all the remaining EEG data from all the channels from all the studies per rat in our analysis

EEG signal analysis - analysis of evoked potentials and frequency specific content

To compute evoked potentials (EP), the EEG time series in the 3–40 Hz band was specifically averaged in response to the ultrasound stimulation across all trials. To reduce noise, the pre-processing band pass filter was a 3–40 Hz 3rd order Butterworth filter. This band removed most of the line noise at 60 Hz (−12 dB at 60 Hz) from the signal, while retaining the part of the rat's brain spectrum where most of the power resides (Leung et al. 1982).

For analysis of evoked potentials before injection of Beuthanasia we used all 200 seconds of data, while for analysis of the post-injection recordings, we used the last set of 200 seconds (last 100 trials), starting typically five to ten minutes after injection of Beuthanasia. This was done to ensure comparison between a pFU activation of a live brain versus a dead one, while maintaining the same experimental conditions (electrode montage, position of US transducer etc.).

To calculate the power at our applied pulse repetition ultrasound frequency of 1050 Hz we first applied a fast Fourier transform (FFT) to the high-pass filtered time series (with a cutoff at 3 Hz), to remove the DC offset from the raw EEG signal. We then applied a Hilbert transform to the narrowband-filtered signal between 1040 Hz and 1060 Hz to compute the trial-to-trial time-varying amplitude of the EEG at 1050 Hz (Tass et al. 1998; Le Van Quyen et al. 2001).

In order to compute an average amplitude time series centered on 1050 Hz, we took the absolute value of the narrowband Hilbert transform at 1050 Hz and averaged it across all trials, following published guidelines (Darvas et al. 2010; Monto et al. 2008).

To compute the entire power spectrum we first split individual trials into separate time series, specifically 1 second prior to turning the pFU on (defined as pFU off), and 1 second while the pFU stimulation is ongoing (defined as pFU on). For each trial and channel, a Hanning window was applied to trial segments separately, and a FFT was computed for pFU-on and pFU-off segments. Spectra were then averaged across all trials, resulting in a pFU-on and pFU-off average spectrum for each channel and rat.

EEG signal analysis - grand average over channels and rats

We computed a grand average over all animals and recorded channels. By averaging over all channels, we eliminate individual spatial variation of any effects within an animal, but we also lose spatial specificity and signal-to-noise ratio (SNR), as we might include channels without any effects in our grand average. As such, this is the most conservative and general approach.

Note that we apply this grand average to computed quantities only, all of which are derived from non-linear transformations (i.e. Z-transform, power spectra, etcetera) from the raw data and thus are not affect by our initial average reference operation.

Since individual animals and channels have variable amplitude/power response to the stimulus, we applied a normalization scheme to each channel in our selection. In case of EPs and computed 1050 Hz amplitude over trials, we used a Z-score transform (Bar et al., 2006) to turn the recorded voltages into a SNR based on the 1 second-long pFU off period in our 2 second-long trial. Specifically, we subtracted the mean-over-time of the signal during the time period from (−1s to 0s, i.e. pFU off) from the total signal, and divided by the standard deviation over time of that signal for that period. In addition to normalizing the amplitude response, the Z-transform also aligns the baseline amplitude to zero. We applied this transform to individual channel averages over trials, before using all normalized channels in the grand average.

EEG signal analysis - spectral ratio and normalization

For the analysis of power spectra we computed the ratio of the power spectra computed during the ‘pFU on’ period divided by the power spectra at that same frequency computed during the ‘pFU off’ period. We did so to accommodate variable noise floor offsets across different channels and animals. These offsets can depend on the particular electrode setup, position of reference, or impedance, but have no direct impact on our hypothesis. Spectral ratios were then turned into Z-scores, as described above, where we used the whole ratio-spectrum to compute a mean and standard deviation across frequencies.

EEG signal analysis - grand average computation

The grand average EP, time-varying 1050 Hz amplitude, and power spectrum were computed from all individual channels and all rats using the respective Z-scores.

EEG signal analysis - analysis of time variation of the 1050 Hz signal after injection

By averaging the 1050 Hz amplitude separately over time during pFU off or on periods within each trial, we computed a single amplitude value for each trial, rat, and condition (pFU on or off, rat pre, or post-injection). From this trial-wise estimate, we constructed a time evolution of the 1050 Hz response of the EEG signal over the course of the experiment with a sampling rate of 1 value every 2 seconds (the combined duration of the pFU off and pFU on period in each trial). Note that the absolute amplitude at 1050 Hz can be substantially influenced by baseline/background noise variation, the particular choice of a reference electrode or individual response in animals to the Beuthanasia injection. Sources of noise for this baseline are likely not of physiological origin, but stem instead from external electrical noise picked up by the montage, most prominently line noise at 60 Hz and its harmonics. This contrasts all other measures and results in this study, which are relative measures comparing pFU on vs. pFU off on short time scales (one second), and are thus invariant to long term (>1s) variations of the baseline. To correct baseline fluctuations in the evolution of the 1050 Hz amplitude, we use the power at 900 Hz (the 15^{th} harmonic of the 60 Hz line noise) as a proxy for any external influences on our EEG signal. Like 1050 Hz, 900 Hz lies well outside the physiological range of neuronal activity that can ordinarily be observed with subdermal needle electrodes outside any event-related setting. Both frequencies fall into the noise floor of the electrode montage and thus have, absent of external influences, the same power. We subtract the 900 Hz amplitude, (estimated in the same way as the 1050 Hz amplitude), from the longer-term time series for the 1050 Hz amplitude, thereby reducing baseline variations. We also smooth both signals (1050 Hz and 900 Hz amplitude) over a period of 1 minute, to eliminate short-term variations, using a thirty sample moving average filter.

Spectrogram calculation and demodulation of the EEG at 1050 Hz

In order to test for the presence of low-frequency modulation of neuronal activity at the pFU stimulation pulse repetition frequency of 1050 Hz, we employed a quadrature amplitude demodulation scheme using Matlab's built in *demod* function on all channels in each rat. We used 1050 Hz, i.e. the pFU stimulation frequency, as the carrier frequency. We applied the demodulation scheme to each trial for both conditions, i.e. pre-injection and post-injection, after band-pass filtering the raw EEG between 1000 Hz and 1100 Hz with a 4^{th} order Butterworth filter, to preserve sufficient bandwidth in the demodulated signal. Here we also used the last 100 trials of stimulation for the post-injection condition. The resultant low frequency signals after demodulation were then used to compute a time frequency spectrogram covering frequencies from 3 to 40Hz in 1 Hz steps for each trial using Morlet wavelets (see e.g. Darvas et al, 2010 for a similar application of the time frequency spectrogram). We computed the absolute value for the complex wavelet coefficients for each trial and took the median across all trials for each animal. We then normalized the spectrogram for each frequency by subtracting a baseline mean, taken over the time period from 1 second prior to the pFU on stimulus to 200 ms before pFU onset and then dividing by the standard deviation over that baseline period. (We did not use the full baseline to avoid edge effects created by use of the wavelet transform.) This produced a normalized SNR estimate for each frequency in the spectrogram. We then applied a two-sided t-test to all 28 channels from 4 rats, where we compared the demodulation spectrogram before and after

injection. We ran a non-parametric permutation test (Bullmore et al, 1999) with cluster-correction, where we permuted the demodulated normalized spectrograms between pre- and post-injection states. We used 10000 permutations, to estimate the maximum cluster distribution under the null hypothesis. The cluster size threshold was set at the 95% percentile of the t-test with 54 degrees of freedom (from 28 channels), i.e. at t=1.67. Note that this test builds a maximum cluster size histogram for the null hypothesis, hence a multiple comparison correction across time and frequency is not required and *p*-levels derived from this test can be considered a correction for false positives.

We applied the same calculations (spectrogram, normalization and permutation test) to the low frequency (3–40 Hz) EEG signal. We did so, however, by excluding the time period from −200 ms to 200 ms flanking the pFU onset from our analysis, as, particularly in the post-injection rat, there is a strong stimulation artifact present in the spectrogram during this time. This artifact could skew the cluster size distribution in our permutation analysis toward larger values. Likewise, we computed and tested a t-statistic between ultrasound on/ultrasound off in the pre-injection rats and in the post-injection rats to test whether any pre/post-injection differences were due to genuine increases of amplitude while the rats were alive.

Results

Alginate Studies - test for EM artifact

Recordings in alginate of stimulation at 1050 Hz without acoustically coupling the pFU transducer to the alginate medium showed no detectable EEG response. Likewise, in a similar study with a rat post-injection, we could not find a detectable EEG response to the pFU stimulation. We therefore conclude that any electromagnetic field that may be created by the ultrasound transducer is not strong enough to affect our recordings.

Alginate Studies - test for non-physiological EEG response to pFU stimulation, *in vitro*

After acoustically coupling the alginate to the transducer, we identified two types of responses to the pFU stimulation. When the electrodes were in the pFU focus, we observed an ‘EP-like’ response (that is, detectable signals in the EP band at 3–40 Hz) at the start and end of the stimulation and a specific response at the ultrasound pulse repetition frequency, i.e. at 1050 Hz (data not shown). With the electrodes in the alginate but outside of the focus, we observed the same EP-like response at the beginning and end of the stimulation persisted, but without any change in EP signal during pFU application, and no noticeable signal at the ultrasound pulse repetition frequency of 1050 Hz. We show an example of this response in Figure 3, where the blue line on the left shows the grand average EP for the alginate pFU stimulation. Due to the 3–40 Hz band pass filter, the EP is smeared out from ~ −100 ms prior to pFU onset to ~ 100 ms post-pFU onset. Another EP, albeit weaker, can be seen at t =1 s, when the pFU is turned off. (The pre-pFU onset part of the EP as observed within alginate is an artifact of the filter, and consistent with its impulse response.) The black lines in the plot indicate two times the standard deviation (95% confidence interval) across channels of the EP. The right panel shows the corresponding narrowband 1050 Hz

amplitude response, averaged across all channels, with the same confidence interval. In all our in-vivo studies, we therefore did not allow the ultrasound to strike the electrodes.

In vivo studies - evoked response in the time domain to pFU stimulation at 3–40 Hz and at 1050 Hz – grand average over all trials, channels, and rats

We calculated a grand average of the normalized average EP, and 1050 Hz amplitude response, where responses for all individual channels for all rats are averaged over all trials. Figure 3 shows the grand average EP (left panel) and the 1050 Hz amplitude response (right panel) for the two states of the rat, i.e. pre-injection (active brain state, orange) and post-injection (inactive brain state, red). Both states in the rat show the EP induced at pFU onset and pFU offset as observed in alginate (blue). There is a location dependence of this EP: it can be more pronounced in particular channels, e.g. to the left and right of the pFU transducer with reversed polarity. Nevertheless, when we split the EP grand average into left/right channels, the EP in the rat remains smaller overall than when observed in the alginate (data not shown). We did not observe any EP averaged over 3–40 Hz other than at pFU–on or pFU–off. We attribute this EP signal at pFU on and off to a stimulation artifact, perhaps due to the net impulsive acoustic radiation force at the beginning and end of the pFU stimulation time (Mourad, 2012) or transient electrical activity by the amplifiers driving the ultrasound.

During the active brain state, we observed a continuous and significant EEG signal at 1050 HZ throughout the period where the pFU stimulation was turned on, which was not present post-injection, during the inactive brain state, nor during baseline measurements, when we did not apply ultrasound.

In vivo studies - transient effects of pFU stimulation during the whole recording period

Representative results of the normalized time series of the amplitude of the 1050 Hz signal for a single channel in each rat are shown in Figure 4. The entire time series of responses shows the evolution of the 1050 Hz amplitude over a time scale of minutes. Prior to injection, all animals exhibited a response in their EEG at 1050 Hz to the ultrasound stimulation, which was consistently higher during pFU-on than during pFU-off periods. This 1050 Hz signal was absent during our baseline recordings, when we did not apply ultrasound. Across all animals, individual responses to the pFU stimulation vary in their dynamic range, covering 16%-49% of the maximum value.

After injection, in all four animals, the pFU-on response, and the pFU-off response converged to a lower overall baseline level than at pFU-on during the pre-injection period. For all animals, pFU-on and pFU-off conditions reached the same baseline level by 10–18 minutes post-injection, although individually the convergence times vary ranging from 220 seconds to 620 seconds post-injection. The overall drop in the pFU-off or baseline level at 1050 Hz can be attributed to the effects of the Beuthanasia acting to inhibit neuronal activity (Random and Barker, 1976), and also to an overall decline in muscle activity, particularly breathing.

In vivo studies - spectral specificity

The grand average normalized ratio spectra shown in Figure 5 demonstrate that the amplitude response to the pFU stimulation was specific to the stimulation frequency of 1050 Hz. These spectra, which integrate the signal over the entire pFU stimulation period and normalize its amplitude by spectral data collected during the entire pFU-off period, also show that post-injection, there still exists a residual effect to the stimulation, albeit greatly reduced in SNR when compared to the effect pre-injection. In both cases, pre- and post-injection, there were harmonics of the stimulation frequency present at 2100 Hz and 3150 Hz, the latter manifesting at 1650 Hz due to wrap-around at the sampling frequency of 4800 Hz. The spectra also show that no event-related synchronization or desynchronization occurred during the whole stimulation time period of 1 second, as we did not observe a significant change in the ratio spectra at typical brain frequencies (below 100 Hz).

In vivo studies - demodulation of the EEG at 1050 Hz

The results of demodulation of the EEG data at 1050 Hz (Figure 6, bottom) demonstrate specific brain activation and inhibition two to three times above and below, respectively, the standard deviation of brain activity present only in the pre-injection state (with $p<0.05$ after global cluster correction) in association with pFU application. These signals have two components, one of activation at gamma frequencies (30–40) Hz and one of inhibition at beta frequencies (17–25 Hz), both starting ~300 ms after the start of pFU stimulation and lasting for ~ 400 ms, specifically ending before cessation of ultrasound application. We find similar gamma activity (but not beta activity) with similar timing within the directly measured low-frequency EEG signal, also shown in Figure 6 (top). In our comparison of pFU-on versus pFU-off in the pre-injection rat (not shown here), we find that the observed increase in gamma power and decrease in beta power are indeed specific to the pre-injection rat brain, rather than due to changes in post-injection rat brain. Since this gamma activity is transient and does not last throughout the whole trial, it does not show up in the grand average spectra (see Figure 5), where activity over the whole stimulation period is integrated over time.

DISCUSSION

With our alginate experiments we showed generation of EEG artifacts - voltage spikes at least ten times that observed at any other time during our study - only when our pFU signal struck an electrode. We also identified an artifact in the EEG signal at the onset and termination of ultrasound stimulation, likely caused by equipment used in the experiment such as the ultrasound amplifiers.

With our *in vivo* experiments we showed generation of a unique, electrophysiological signal within rat brain at a frequency of 1050 Hz, detectable only during delivery into living brain of ultrasound pulses at that same pulse repetition frequency (PRF) (Figures 3–5). In rats, single neurons have demonstrated an absolute refractory period of approximately 1 ms, meaning a maximum firing rate on the order of 1kHz (Rolls, 1970). This compares favorably with our PRF, which is equal to the induced high-frequency electrophysiological signal. After animals were injected with Beuthanasia, the amplitude of the 1050 Hz signal

decreased over time as the animal died (Figure 4). Spectral analysis of the electrical activity showed that the 1050 Hz signal was dominant over natural brain activity in pre-injection animals; post-injection animals supported a weaker, and diminishing 1050 Hz signal (Figure 5). From this we conclude that generation of an optimal 1050 Hz electrophysiological signal requires delivery of pulses of pFU into living brain.

We also observed brain activity within approximately beta and gamma frequency bands after demodulation of the directly measured high frequency (1050 Hz) EEG signal (Figure 6, bottom), commensurate with directly measured gamma activity (Figure 6, top). This finding suggests that in the pre-injection rat, pFU application at a PRF of 1050 Hz modulated low-frequency endogenous brain activity and/or directly evoked brain rhythms in these low-frequency bands. In contrast, however, we did not observe an evoked potential associated with pFU stimulation, beyond a small residual stimulation artifact (Figure 3). Taken together, these results support the view that the low-frequency (beta, gamma) inhibition and activation, respectively, correlated in a delayed fashion with the pFU stimulation at 1050 Hz. With regard to the delay, we note that similar observations exist in relation to sensorimotor tasks in human studies (Miller et al. 2007; Fuerra et al. 2011) and in non-human primates (Murray et al, 2014). The results of these earlier studies and our observations suggest the high-frequency pFU stimulus induced or modulated low-frequency brain activity and inhibition associated with the thalamocortical network (Douglas and Martin, 1991; Wang et al., 2011; Sun et al., 2006; Vianney-Rodrigues et al., 2011) although other neural circuits can display a similar delay (e.g., Wang et al., 2011). Mueller et al. (2014) report that transcranially delivered focused ultrasound to humans can modulate the phase and phase rate but not the amplitude of intrinsic beta (but not gamma) activity bands. They also note a difference between beta and gamma power for late somatosensory evoked potentials (SEPs) (71–260ms), but not for early SEPs (17–70ms). The former is approximately when we see the amplitudes of beta and gamma beginning to change in the rat brain activity, though the neurophysiology will not be exactly the same.

One can plausibly hypothesize that any low-frequency EEG signals derived via demodulation of the high-frequency 1050 Hz EEG signal originates from within the focal volume of pFU. This hypothesis (if supported by future work, see below) is consistent with the observations of the Tyler group (Legon et al., 2014; Mueller et al., 2014) who saw changes in gamma band activity in humans undergoing sensory stimulation only when they targeted focused ultrasound to within 1 centimeter of S1, part of the sensorimotor cortex. Similarly, Deffieux et al. (2013) observed that their induction of antisaccade latencies in primates by application of focused ultrasound to the brains of non-human primates disappeared once the ultrasound focus was moved away from the targeted frontal eye field by a comparable amount.

LIMITATIONS

In Mehić et al (2014), we used a pulse repetition frequency (1500 Hz) comparable to that used here (1050 Hz) to generate externally observable behavioral responses to brain stimulation by transcranially delivered pFU. Our choice here of a pulse repetition frequency of 1050 Hz allowed us to generate a signal outside the natural frequency range of neuronal

firing, within the duration and refractory period of action potentials within the brain (Kandel et al., 2000; Gittis et al., 2010; Buzsaki and Draguhn, 2004), and measurable by our EEG system, all while avoiding frequencies associated with our electronic equipment (multiples of 60 Hz). It will be of interest in future studies to see if we can generate electrophysiological signals above the natural time scale of action potentials within brain. We predict that a sufficiently high value of pulse repetition frequency for pFU stimulation would lead to rapidly depleted signals in living brain, as the stimulated neurons lose their capacity to fire through depletion of their internal stores of calcium and sodium.

Future work should include use of a larger brained animal to quantify how deep into brain we can project pFU and still detect a pFU-induced electrophysiological signal. It would also allow us to aim at and monitor primarily white or primarily gray matter, unlike in the rat. Also, given the increase in spontaneous EEG bursts in the cortex and their decrease in the thalamus through use of isoflurane as an anesthetic (Detsch et al., 2002), it will also be of interest to aim ultrasound at superficial (e.g., cortical) versus deep (e.g., thalamic) portions of brain to see if there exist different thresholds for brain activation induced by ultrasound associated with this difference in intrinsic activity.

Future efforts should also build on these first studies to directly address the long-term goal of this work: production of an identifiable tag of endogenous electrophysiological activity within a small focal volume of brain, without any effect on that activity. As an example of such a test, one might use an animal model of known focal brain activity, such as epilepsy (Sobayo and Mogul, 2013) or visual stimulation (Yoo et al 2011), in effect, a positive control. With subdermal electrodes in place in a model of epilepsy, for example, one would monitor the focal epileptic activity with and without application of pFU to the epileptic nidus as well as to epilepsy-free brain tissue, available during the early time course of epileptic activity in this model. Only with application of pFU to the epileptic nidus would we expect to observe coupled EP and stimulation frequencies. Methods for detection of this kind of coupling in cortical signals have already been established (Darvas et al., 2009).

With regard to the safety of ultrasound-mediated neuromodulation, we note that there exist two recent studies demonstrating neuromodulatory effects of transcranially delivered ultrasound on humans (Legon et al., 2014; Lee et al., 2015) while another study demonstrated comparable effects on non-human primates (Deffieux et al., 2013), all without adverse events. Of interest, these ultrasound protocols made use of ultrasound delivered at frequencies below those covered by FDA guidelines (0.5 MHz, 0.25 MHz, 0.32 MHz, respectively), with a range of estimated transcranial intensities (2.2 W/cm^2, 0.35 W/cm^2, 0.014 W/cm^2, all I_spta) relative to the FDA guidelines for an upper bound on intensity for diagnostic ultrasound (0.72 W/cm^2 I_spta; defined at and above 1 MHz and after derating for attenuation through intervening tissue). Also relevant, these ultrasound protocols lie well below that used without acoustic contrast agents to create blood-brain barrier disruption (again, see Mesiwala et al., 2002), a relatively subtle form of brain-tissue damage. These successful (efficacious; safe) ‘first in primate’ studies will motivate more human subjects-based research, always with careful attention to safety, as evidenced by the care taken by the authors of the research cited above and at least because of the unfortunate results of Daffertshofer et al. (2005) whose low-frequency ultrasound (300 kHz) plus, importantly,

tissue plasminogen activator injected with non-degassed fluid, induced a significant incidence of intracerebral hemorrhage in stroke patients relative to controls.

Finally, with regard to mechanisms by which ultrasound may interact with brain, this remains an open question (Tyler, 2012), one unaddressed by this paper. Here we consider two possible mechanisms beyond those discussed by Tyler (2012). We note that a propagating action potential can produce volumetric changes in the axon carrying that potential (e.g., Iwasa and Tasaki, 1980). One may describe this as a 'piezoelectric' effect, since piezoelectric ceramics used to build ultrasound transducers change volume when subjected to an electric field (Mourad, 2012). Furthermore dendritic spines twitch and contract rapidly as a result of action potential propagation. One may therefore hypothesize a mechanism of ultrasound's activation of brain as a 'converse' piezoelectric effect: mechanical pressure induced by the ultrasound's acoustic radiation force averaged over a pulse may compress a small volume of brain tissue, including its axons and/or synapses, at the pulse repetition frequency of the ultrasound (again, 1050 Hz here), resulting in a redistribution of charges, ion channel activity and/or neurotransmitter release which then produces an electrical signal from within that location. (Note again that this by analogy to how piezoelectric ceramics work: pressure waves incident upon such a ceramic distort the ceramic, thereby inducing an electric current within the ceramic capable of conducting from the ceramic.) An alternative physical mechanism to explain the observed signals is the acousto-electro effect (Fox et al., 1946, Jossinet et al., 1999), which relates changes in conductivity of electrically charged material (e.g., salt water), due to an ultrasound pressure field passing through that material, here at the carrier frequency of 2 MHz. Local conductivity changes might lead to the type of amplitude modulation that we have found in our data, under the assumption that a large enough ensemble of active neurons acts as a constant current source in that volume. Recent studies (Yang et al., 2012) have also shown in a related application (electrical impedance tomography coupled with ultrasound) that the magnitude of the effect can depend upon the ultrasound pulse shape. Future work should therefore include optimization of brain activation through alteration of the ultrasound pulse waveform as well as changes in the pulse repetition frequency, carrier frequency, and intensity.

CONCLUSION

Current non-invasive technology cannot unambiguously record electrophysiological activity from within focal and deep brain structures in humans (e.g., for epilepsy localization) and non-human primates (e.g., for fundamental studies of brain function). As a first step towards rectifying this circumstance, we have demonstrated here that transcranial application of pulsed focused ultrasound (pFU) to rat brain can generate a unique high-frequency electrophysiological signal detectable extra-cranially from which we derived plausible measures of low-frequency, likely focal brain activity. Future work will directly test the hypothesis motivating our work - that we can use this unique signal to 'tag' endogenous brain activity within and only within the focal volume of the pFU that generates the unique electrophysiological signal.

Furthermore, we note that application of pFU (or modulated focused ultrasound) using the same device but with different, though readily accessible acoustic parameters can alter focal brain function (Mehić et al., 2014). This is consistent with other groups using focal ultrasound to stimulate a focal region of brain (Yoo et al., 2011, King et al., 2014, Legon et al., 2014, Mueller et al., 2014)). Interestingly, such alteration of brain function does not induce electrophysiological artifacts in EEG systems (Tyler et al., 2008; Tufail et al., 2010, 2011), unlike electrically induced modulation of brain function. Moreover, there already exist clinical systems for delivery of focal ultrasound, under MRI guidance, that can insure the focus of the ultrasound survives distortion, allowing us to precisely localize a known volume and shape of ultrasound within a portion of desirable brain tissue (Marsac et al., 2012). Utilizing the focal nature of the modulated volume and a precise knowledge of the head geometry and electrode locations (which is commonly employed in human EEG analysis), a multi channel, typically 64 channel electrode setup could be expected to improve on the SNR by using a focal beamforming algorithm, among other techniques. Therefore, the work presented here, along with published work on ultrasound modulation of brain function, suggests that we can anticipate creation of a completely closed-loop brain-computer interface with real-time monitoring and control of brain function, all based on non-invasive monitoring of brain function (via EEG plus pFU) and alteration of brain function at least at the pulse repetition frequency of pFU or mFU.

Acknowledgments

All work and assistance on this project is directly associated with the listed authors. Jeff Ojemann and Felix Darvas were supported by NIH (R01NS065186). Felix Darvas was also supported by NIH (R01MH094366). Funding for Pierre D. Mourad, Edin Mehić, and Connor Caler was provided by the University of Washington's Center for Commercialization via its Entrepreneurial Faculty Fellow's grant. We thank Tessa Olmstead for her critical reading of the manuscript and Nathan Coulson for making transcranial measurements of ultrasound. We thank the reviewers of this manuscript whose constructive comments significantly improved this paper.

References

Arenkiel B, Peco J, Davison I, Feliciano C, Deisseroth K, Augustine G, Ehlers M, Feng G. In vivo light-induced activation of neural circuitry in transgenic mice expressing channelrhodopsin-2. Neuron. 2007; 54:205–218. [PubMed: 17442243]

Ball T, Demandt E, Mutschler I, Neitzel E, Mehring C, Vogt K, Aertsen A, Schulze-Bonhage A. Movement related activity in the high gamma range of the human EEG. NeuroImage. 2008; 41(2): 302–310. [PubMed: 18424182]

Ballantine HT, Bell E, Manlapaz J. Progress and Problems in the Neurological Applications of Focused Ultrasound. Journal of Neurosurgery. 1960; 17(5):858–876. [PubMed: 13686380]

Bar M, Kassam KS, Ghuman AS, Boshyan J, Schmid AM, Dale AM, Hämäläinen MS, Marinkovic K, Schacter DL, Rosen BR, Halgren E. Top-down facilitation of visual recognition. Proc. Natl. Acad. Sci. 2006; 103:449–454. [PubMed: 16407167]

Bullmore ET, Suckling J, Overmeyer S, Rabe-Hesketh S, Taylor E, Brammer MJ. Global, voxel, and cluster tests, by theory and permutation, for a difference between two groups of structural MR images of the brain. Med. Imaging, IEEE Trans. 1999; 18:32–42.

Buzsaki G, Draguhn A. Neuronal Oscillations in Cortical Networks. Science. 2004; 304:1926–1929. [PubMed: 15218136]

Cheyne D, Bells S, Ferrari P, Gaetz W, Bostan AC. Self-paced movements induce high-frequency gamma oscillations in primary motor cortex. NeuroImage. 2008; 42(1):332–42. [PubMed: 18511304]

Daffertshofer M, Gass A, Riungleb P, Sitzer M, Sliwka U, Ells T, Sedlaczek O, Koroshetz W, Hennerici MG. Transcranial low-frequency ultrasound-mediated thrombolysis in brain ischemia. Stroke. 2005; 36:1441–1446. [PubMed: 15947262]

Darvas F, Hebb AO. Task specific inter-hemispheric coupling in human subthalamic nuclei. Front Hum Neurosci. 2014; 8(701)

Darvas F, Scherer R, Ojemann JG, Rao RP, Miller KJ, Sorensen LB. High gamma mapping using EEG. NeuroImage. 2010; 49(1):930–938. [PubMed: 19715762]

Darvas F, Pantazis D, Kucukaltun-Yildirim E, Leahy RM. Mapping human brain function 659 with MEG and EEG: Methods and validation. NeuroImage. 2004; 23(Suppl 1):S289–99. [PubMed: 15501098]

Darvas F, Rao RPN, Murias M. Localized high gamma motor oscillations respond to perceived biologic motion. Journal of clinical neurophysiology: official publication of the American Electroencephalographic Society. 2013; 30(3):299–307. [PubMed: 23733096]

Darvas F, Miller KJ, Rao RPN, Ojemann JG. Nonlinear phase-phase cross-frequency coupling mediates communication between distant sites in human neocortex. The Journal of Neuroscience. 2009; 29(2):426–435. [PubMed: 19144842]

Darvas F, Scherer R, Ojemann JG, Rao RP, Miller KJ, Sorensen LB. High gamma mapping using EEG. Neuroimage. 2010; 49(1):930–938. 2010. [PubMed: 19715762]

Darvas F, Ojemann JG, Sorensen LB. Bi-phase locking - a tool for probing non-linear interaction in the human brain. NeuroImage. 2009; 46(1):123–132. [PubMed: 19457390]

Dalal SS, Guggisberg AG, Edwads E, Sekihara K, Findlay AM, Canolty RT, Berger MS, Knight RT, Barbaro NM, Kirsch HE, Nagarajan SS. Five-dimensional neuroimaging: localization of the time-frequency dynamics of cortical activity. NeuroImage. 2008; 40(4):1686–1700. [PubMed: 18356081]

Daffertshofer M, Gass A, Ringleb P, Sitzer M, Sliwka U, Els T, Sedlaczek O, Koroshetz WJ, Hennerici MG. Transcranial Low-Frequency Ultrasound-Mediated Thrombolysis in Brain Ischemia: Increased Risk of Hemorrhage With Combined Ultrasound and Tissue Plasminogen Activator: Results of a Phase II Clinical Trial. Stroke. 2005; 36:1441–1446. [PubMed: 15947262]

Deffieux T, Younan Y, Wattiez N, Tanter M, Pouget P, Aubry J. Low-Intensity Focused Ultrasound Modulates Monkey Visuomotor Behavior. Current Biology. 2013; 23(23):2430–2433. [PubMed: 24239121]

Detsch O, Kochs E, Siemers M, Broom B, Vahle-Hinz C. Increased responsiveness of cortical neurons in contrast to thalamic neurons during isoflurane-induced EEG bursts in rats. Neuroscience Letters. 2002; 317(1):9–12. [PubMed: 11750984]

Douglas R, Martin K. A functional microcircuit for cat visual cortex. Journal of Physiology. 1990; 440:735–769. 1990.

Fedele T, Scheer HJ, Burghoff M, Curio G, Korber R. Ultra-low-noise EEG/MEG systems enable bimodal non-invasive detection of spike-like human somatosensory evoked responses at 1 kHz. Physiological measurement. 2015; 36(2):357–68. [PubMed: 25612926]

Fish RE. Anesthesia and Analgesia in Laboratory Animals. Amsterdam: Academic. 2008

Fox F, Herzfeld K, Rock G. The effect of ultrasonic waves on the conductivity of salt solutions. Physical Reviews. 1946; 70:329–339.

Fry WJ. Electrical Stimulation of Brain Localized without Probes-Theoretical Analysis of a Proposed Method. The Journal of the Acoustical Society of America. 1968; 44(4):920–931.

Fry WJ. Use of Intense Ultrasound in Neurological Surgery Research. Am J Phys Med. 1958; 37(3): 143–47. [PubMed: 13545380]

Fuerra M, Bianco G, Santarnecchi E, Testa M, Rossi A, Rossi S. Frequency-Dependent Tuning of the Human Motor System Induced by Transcranial Oscillatory Potentials. The Journal of Neuroscience. 2011; 31:12165–12170. [PubMed: 21865459]

Gittis AH, Moghadam SH, Du Lac S. Mechanisms of Sustained High Firing Rates in Two Classes of Vestibular Nucleus Neurons: Differential Contributions of Resurgent Na, Kv3, and BK Currents. Journal of Neurophysiology. 2010; 104(3):1625–634. [PubMed: 20592126]

Gevins A, Yeager C, Zeitlin G, Ancoli S, Dedon M. On-Line Computer Rejection of EEG Artifact. Electroencephalography and Clinical Neurophysiology. 1997; 42:267–274.

Iwasa K, Tsaki I. Mechanical changes in squid giant axons associated with production of action potentials. Biochemical and Biophysical Research Communications. 1980; 95(3):1328–1331. [PubMed: 7417318]

Jossinet J, Lavandier B, Cathignol D. Impedance Modulation by Pulsed Ultrasound. Annals of the New York Academy of Sciences. 1999; 873:396–407.

Kandel, ER., Schwartz, JH., Jessell, TM. Principles of Neural Science. New York: McGraw-Hill, Health Professions Division; 2000.

King RL, Brown JR, Newsome WT, Pauly KB. Effective parameters for ultrasound-induced in-vivo neurostimulation. Ultrasound Med Biol. 2013; 39(2):312–331. [PubMed: 23219040]

King RL, Brown JR, Pauly KB. Localization of Ultrasound-Induced In Vivo Neurostimulation in the Mouse Model. Ultrasound in Medicine & Biology. 2014; 40(7):1512–22. [PubMed: 24642220]

Le Van Quyen M, Foucher J, Lachaux J, Rodriguez E, Lutz A, Martinerie J, Varela FJ. Comparison of Hilbert transform and wavelet methods for the analysis of neuronal synchrony. Journal of Neuroscience Methods. 2001; 111(2):83–98. [PubMed: 11595276]

Legon W, Sato TF, Opitz A, Mueller J, Barbour A, Williams A, Tyler WJ. Transcranial focused ultrasound modulates the activity of primary somatosensory cortex in humans. Nature Neuroscience. 2014; 17:322–329. [PubMed: 24413698]

Leung LWS, Da Silva FHL, Wadman WJ. Spectral characteristics 721 ics of the hippocampal 722 EEG in the freely moving rat. Electroencephalogr. Clin. Neurophysiol. 1982; 54(2):203–219.

Maganti RK, Rutecki P. EEG and Epilepsy Monitoring. CONTINUUM: Lifelong Learning in Neurology. 2013; 19(3):598–622. [PubMed: 23739100]

Marsac L, Chauvet D, Larrat B, Pernot M, Robert B, Fink M, Boch AL, Aubry JF, Tanter M. MR-guided Adaptive Focusing of Therapeutic Ultrasound Beams in the Human Head. Medical Physics. 2012 39.2.

Megevand P, Troncoso E, Quairiaux C, Muller D, Michel C, Kiss J. Long-term plasticity in mouse sensorimotor circuits after rhythmic whisker stimulation. The Journal of Neuroscience. 2009; 29:5326–5335. [PubMed: 19386929]

Mehić E, Xu JM, Caler CJ, Coulson NK, Moritz CT, Mourad PD. Increased Anatomical Specificity of Neuromodulation via Modulated Focused Ultrasound. PLoS ONE. 2014; 9(2)

Mesiwala AH, Farrell L, Wenzel HJ, Crum LA, Silbergeld DL, Winn HR, Mourad PD. High Intensity Focused Ultrasound Selectively Disrupts the Blood-Brain Barrier in vivo. Ultrasound in Medicine and Biology. 2002; 28(1):389–400. [PubMed: 11978420]

Miller K, Leuthardt E, Schalk G, Rao R, Anderson N, Moran D, Miller J, Ojemann J. Spectral Changes in Cortical Surface Potentials during Motor Movement. The Journal of Neuroscience. 2007; 27:2424–32. [PubMed: 17329441]

Monto S, Palva S, Voipio J, Palva JM. Very Slow EEG Fluctuations Predict the Dynamics of Stimulus Detection and Oscillation Amplitudes in Humans. J. Neurosci. 2008; 28(33):8268–8272. [PubMed: 18701689]

Mourad, PD. Therapeutic Ultrasound, with an emphasis on applications to the brain. In: Nakamura, K., Ueha, S., editors. Ultrasonic transducers - Materials Design and Applications. Woodhead Publishing Ltd; 2012. p. 545-568.

Mueller J, Legon W, Opitz A, Sato TF, Tyler WJ. Transcranial focused ultrasound modulates intrinsic and evoked EEG dynamics. Brain Stimulation. 2014; 7:900–908. [PubMed: 25265863]

Murray JD, Bernacchia A, Freedman DJ, Romo R, Wallis JD, Cai X, Padoa-Schioppa C, Pasternak T, Seo H, Lee D, Wang XJ. A hierarchy of intrinsic timescales across primate cortex. Nature Neuroscience. 2014; 17(12)

Myers MR. Tissue deformation induced by radiation force from Gaussian transducers. J. Acoust. Soc. Am. 2006; 119:3147–3152. [PubMed: 16708969]

Nightingale K. Acoustic Radiation Force Impulse (ARFI) Imaging: a Review. Curr Med Imaging Rev. 2012; 7(4):328–339.

Ransom BR, Barker JL. Pentobarbital selectively enhances GABA-mediated post-synaptic inhibition in tissue cultured mouse spinal neurons. Brain Res. 1976; 114(3):530–535. [PubMed: 953775]

Rolls E. Absolute refractory period of neurons involved in MFB self-stimulation. Physiology and behavior. 1970; 7:311–315.

Smith MM, Weaver KE, Grabowski TJ, Rao RP, Darvas F. Non-invasive detection of high gamma band activity during motor imagery. Frontiers in Human Neuroscience. 2014; 8:817. [PubMed: 25360100]

Sobayo T, Mogul DJ. Rapid onset of a kainate-induced mirror focus in rat hippocampus is mediated by contralateral AMPA receptors. Epilepsy Res. 2013; 106(1–2):35–46. [PubMed: 23668947]

Sun J, Yang J, Shyu B. Current source density analysis of laser-heat evoked intra-cortical field potentials in the primary somatosensory cortex of rats. Neuroscience. 2006; 140:1321–1336. [PubMed: 16675140]

Tass P, Rosenblum MG, Weule J, Kurths J, Pikovsky A, Volkmann J, Schnitzler A, Freund H-J. Detection of n:m Phase Locking from Noisy Data: Application to Magnetoencephalography. Physical Review Letters. 1998; 81(15):3291–3294.

Telenczuk B, Baker SN, Herz AV, Curio G. High-frequency EEG covaries with spike burst patterns detected in cortical neurons. Journal of neurophysiology. 2011; 105(6):2951–9. [PubMed: 21490283]

Teleńczuk B, Baker SN, Kempter R, Curio G. Correlates of a single cortical action potential in the epidural EEG. NeuroImage. 2015; 109:357–67. [PubMed: 25554430]

Tufail Y, Matyushov A, Baldwin N, Tauchmann ML, Georges J, Yoshihiro A, Tillery SIH, Tyler WJ. Transcranial Pulsed Ultrasound Stimulates Intact Brain Circuits. Neuron. 2010; 66(5):681–694. [PubMed: 20547127]

Tufail Y, Yoshihiro A, Pati S, Li MM, Tyler WJ. Ultrasonic neuromodulation by brain stimulation with transcranial ultrasound. Nature Protocol. 2011; 6(9):1453–1470.

Tyler WJ, Tufail Y, Finsterwald M, Tauchmann ML, Olson EJ, Majestic C. Remote Excitation of Neuronal Circuits Using Low-Intensity, Low-Frequency Ultrasound. PLoS ONE. 2008; 3(10)

Vianney-Rodrigues P, Iancu O, Welsh J. Gamma Oscillations in the Auditory Cortex of Awake Rats. Eur. J. Neurosci. 2014; 33:119–129.

Vykhodtseva NI, Koroleva VI. Changes in the steady potential in various structures of the rat brain induced by focused ultrasound. Dokl Akad Nauk SSSR. 1986; 287(1):248–51. [PubMed: 3956374]

Wang J, Li D, Li X, Liu F, Xing G, Cai J, Wan Y. Phase-amplitude coupling between theta and gamma oscillations during nociception in rat electroencephalography. Neuroscience Letters. 2011; 499:84–87. [PubMed: 21640788]

Wennberg R, Cheyne D. EEG Source Imaging of Anterior Temporal Lobe Spikes: Validity and Reliability. Clinical Neurophysiology. 2013; 125(5):886–902. [PubMed: 24210516]

Yang R, Li X, Song A, He B, Yan R. Three-dimensional noninvasive ultrasound Joule heat tomography based on the acousto-electric effect using unipolar pulses: a simulation study. Physics in Medicine and Biology. 2012; 57(22):7689–7708. [PubMed: 23123757]

Yang X, Hyder F, Shulman RG. Activation of single whisker barrel in rat brain localized by functional magnetic resonance imaging. Proc. Natl. Acad. Sci. 1996; 93:475–478. [PubMed: 8552664]

Yoo SS, Bystritsky A, Lee JH, Zhang Y, Fischer K, Min BK, Mcdannold NJ, Pascual-Leone A, Jolesz FA. Focused Ultrasound Modulates Region-specific Brain Activity. NeuroImage. 2011; 56(3): 1267–275. [PubMed: 21354315]

Younan Y, Deffieux T, Larrat B, Fink M, Tanter M, Aubry JF. Influence of the pressure field distribution in transcranial ultrasonic neurostimulation. Medical physics. 2013; 40(8):082902.doi: 10.1118/1.4812423 [PubMed: 23927357]

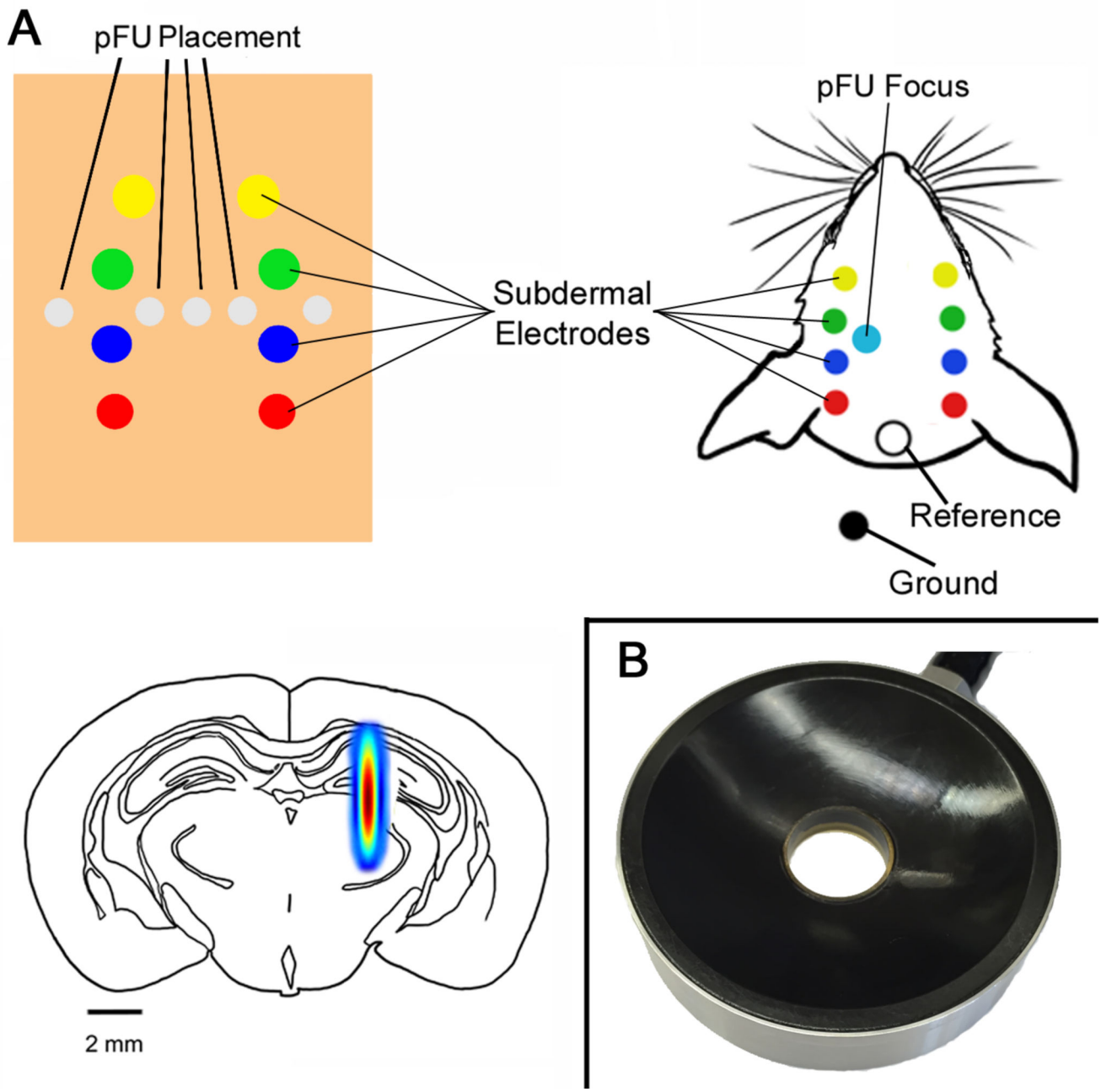

Figure 1. Ultrasound and EEG placement

(Upper Left) Diagram of the alginate experiment, demonstrating placement of EEG electrodes and the ultrasound focus within alginate gel. (Upper right) Diagram of the *in vivo* experiment, showing placement of the ultrasound focus, recording and reference EEG electrodes, all relative to the surface of the rat head. We placed the ground on the shoulder of the rat. (Lower Left) Schematic of a coronal slice of rat brain showing the ultrasound focus within rat brain, to scale. The full spectrum of the ultrasound focus represents the full width half maximum pressure (modified from Mehić et al., 2014). (Lower Right) Photograph of the ultrasound transducer we used to stimulate brain with pulsed focused ultrasound.

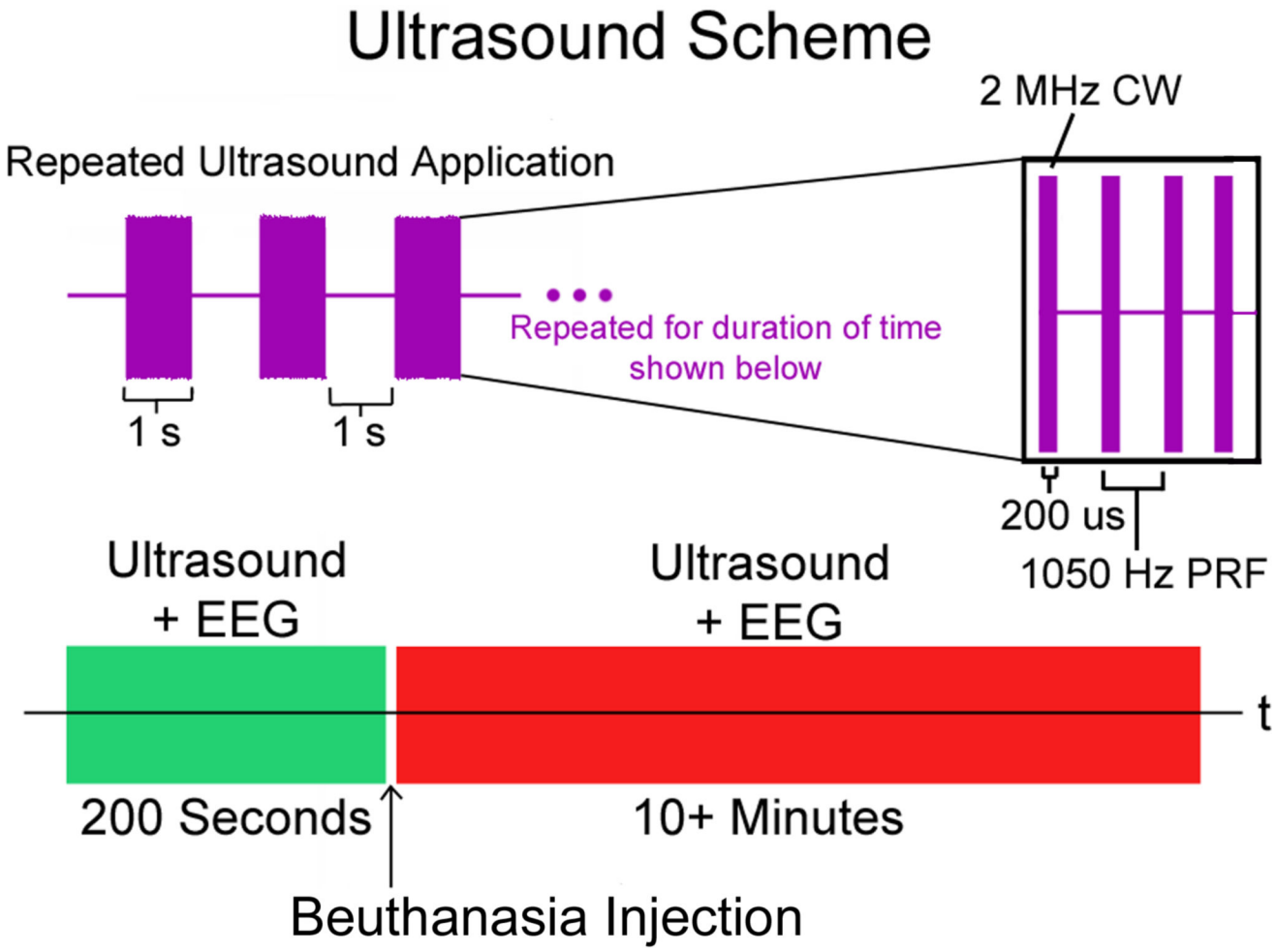

Figure 2. Schematic of ultrasound protocol

In purple we show constant wave (CW) ultrasound pulses each lasting for 200 μs based on a 2 MHz carrier frequency and a pulse repetition frequency (PRF) of 1050 Hz. This pattern lasts for one second, followed by a one second period with no ultrasound. This on/off period (in green) lasts for 100 repetitions (200 seconds) during which EEG is continuously recorded. This is immediately followed by a Beuthanasia injection lasting approximately 30 seconds followed immediately by continued ultrasound application and EEG recording as above for approximately 10 minutes (in red).

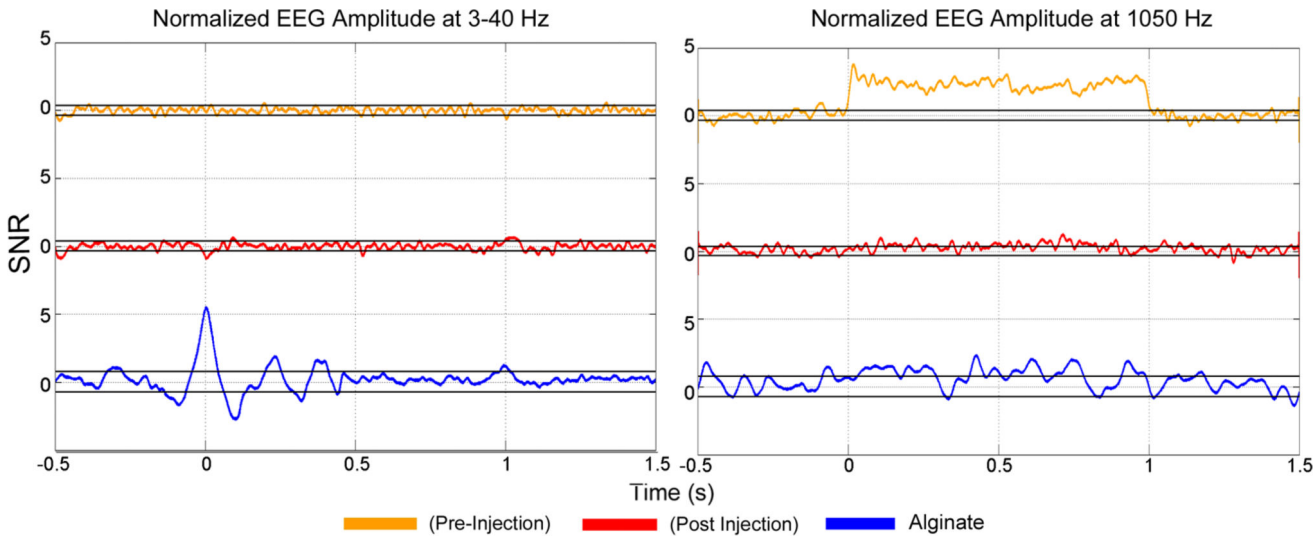

Figure 3. Normalized EEG amplitude responses

Grand average evoked potentials (EP) in the 3–40 Hz band (left) and 1050 Hz amplitude response (right) over the course of the two second long pFU off/on trial. The time course shown is from 0.5 s prior to pFU stimulation to 1.5 s after pFU stimulation, to allow us to illustrate pFU-stimulation onset and offset effects. Shown are data from alginate (blue), before injection of Beuthanasia ('pre-injection', in green) and after injection of Beuthanasia ('post injection', in red), in units of SNR relative to the 'pFU-off' period. Black lines for each graph indicate the 99.5% confidence intervals. Note that the EP are shown as an SNR of measured voltage averaged over 3–40 Hz, while the 1050 Hz response is shown as the SNR of the amplitude of the band pass filtered voltage between 1040 and 1060 Hz.

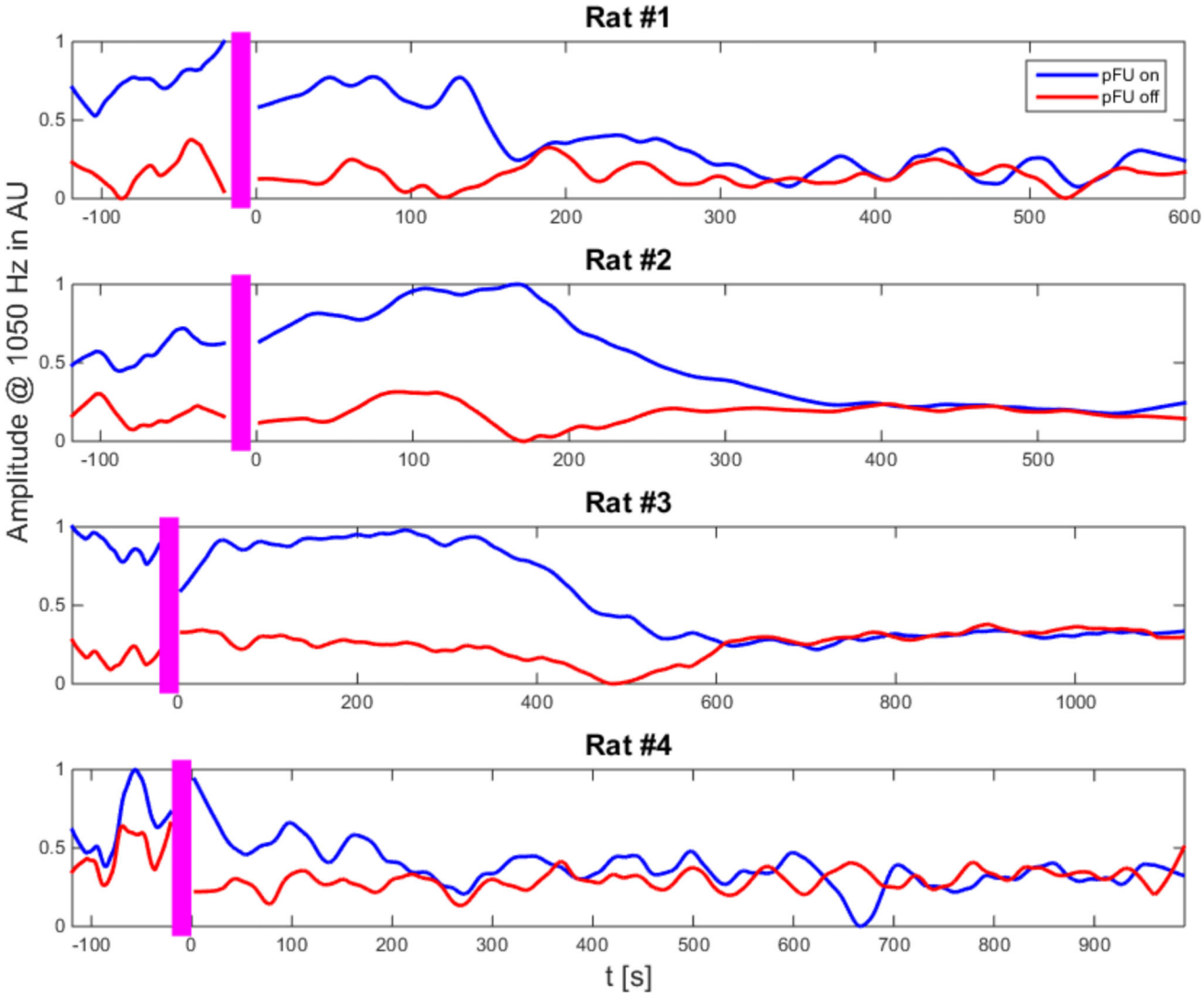

Figure 4. Time course of EEG signal at 1050 Hz

Representative time course of the integrated 1050 Hz amplitude from a single channel for each rat in our study. The blue curve shows the response during the one-second pFU-on period, the red curve the corresponding EEG-derived 1050 Hz amplitude during the one-second pFU-off period. (Note that during the actual experiment we alternated between 'pFU-on' for one second and 'pFU-off' for one second). Both 1050 Hz amplitude curves have been scaled to their common maximum value and have been smoothed with a moving average filter of one minute in duration. The noise floor measured at 900 Hz has also been subtracted from each signal. The x-axis shows the time in seconds. Here time before zero indicates time before injection of Beuthanasia, the time under anesthesia but otherwise 'active' brain. The time after zero indicates the time after injection of Beuthanasia, the time of an 'inactive' brain state. Pre– and post– injection time periods are separated by the pink bar. We use the EEG data from the last 100 seconds of the post-injection time period in the analysis of Figures 3 and 5.

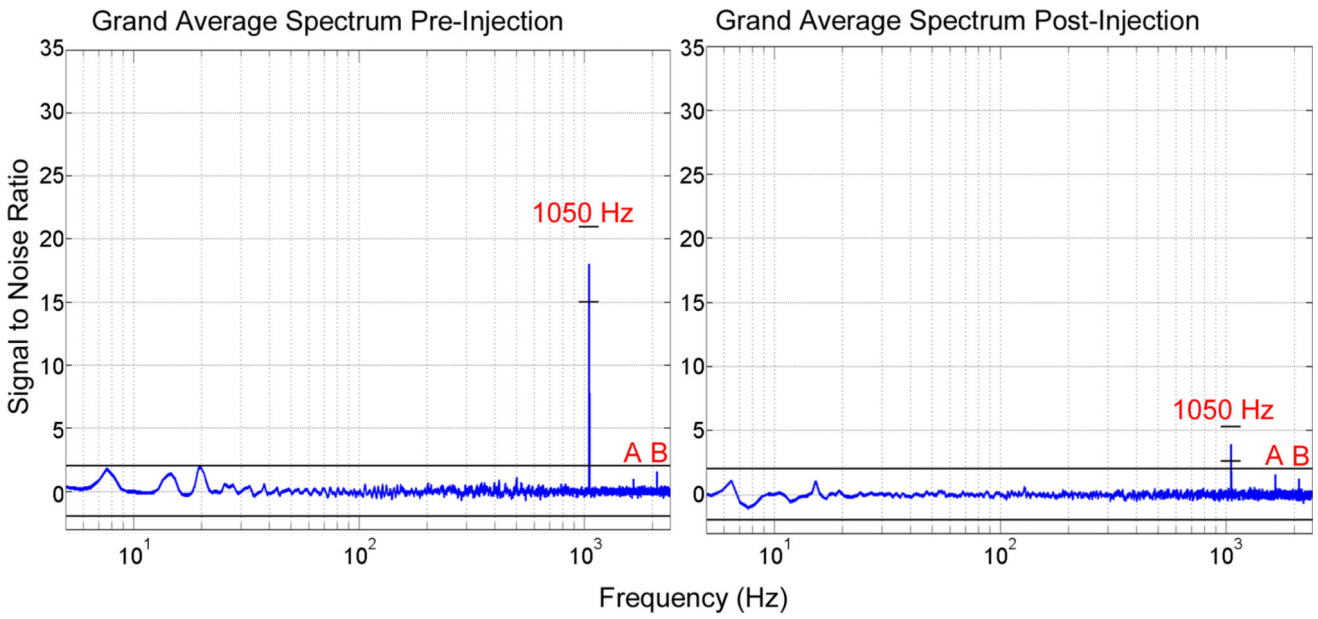

Figure 5. EEG average spectra

Grand average of the normalized ratio spectrum between pFU-on and pFU-off conditions for all channels from all rats. The spectrum for the pre-injection state is shown on the left, for the post injection state on the right. The X-axis is a log-scale of frequencies, ranging from 5 Hz to 2000 Hz. The SNR value at the stimulation frequency in both states is annotated and shown with the frequency-specific 99.5 % confidence interval (small black lines around the 1050 Hz peak). Otherwise the black lines indicate the confidence interval across all frequencies. The peaks annotated with (A) and (B) are located at, respectively, 2100 Hz (1st harmonic of 1050 Hz) and 1650 Hz (a wrap-around of 3150 Hz, i.e. 3rd harmonic of 1050 Hz, which occurs due to our limited sampling frequency of 4800 Hz).

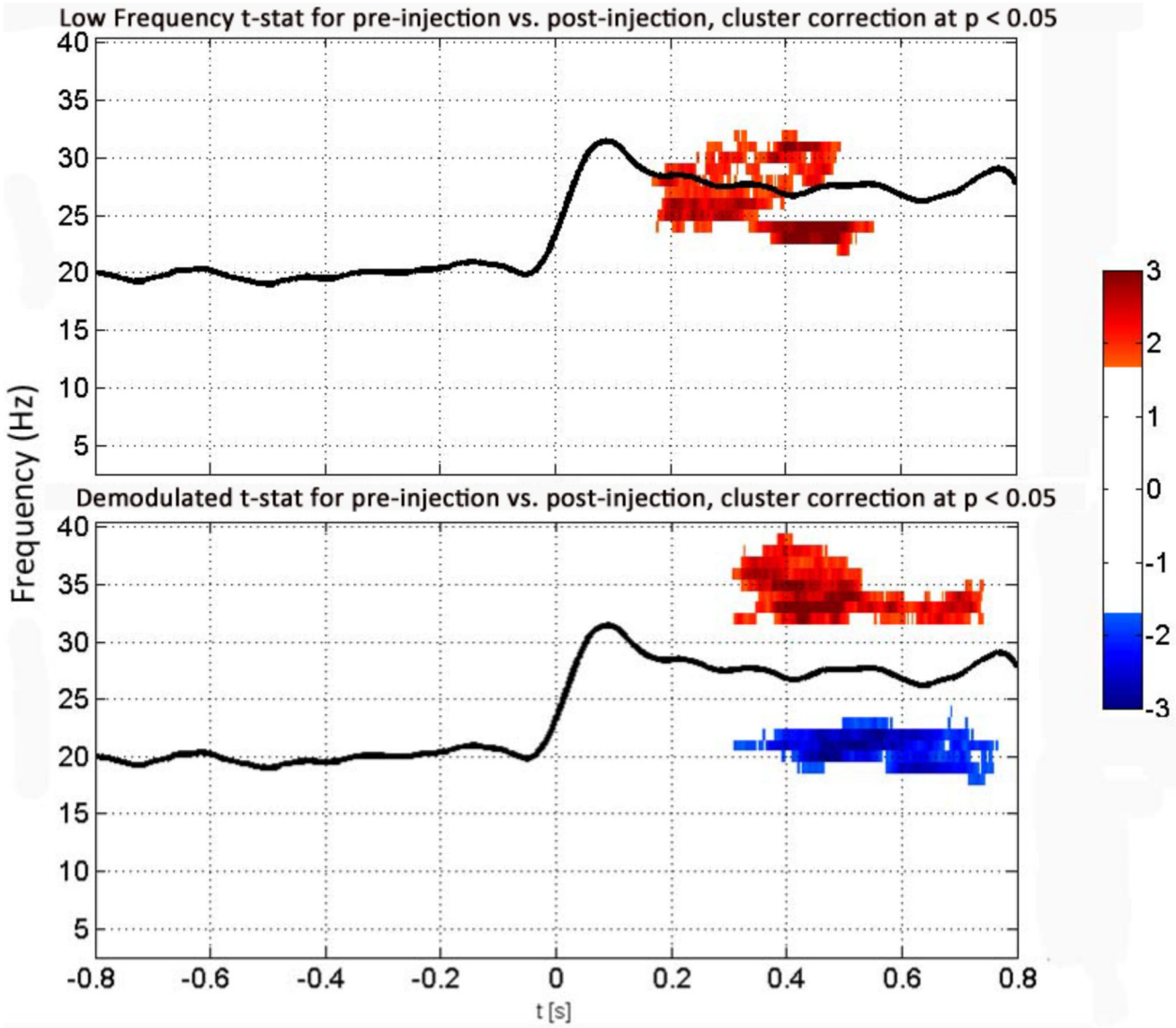

Figure 6. Directly measured low frequency spectrogram versus demodulated high-frequency spectrogram

Grand average t-test results of the spectrograms of the low frequency (3-40 Hz) (top) and demodulated high frequency (1050 Hz, bottom) EEG for all channels (eight) for all rats (four), pre-injection. We have normalized these measurements by the same measures collected from each animal during the last 100s post-injection. The x-axis shows time in seconds, with t = 0 s indicating the start of the pFU-on and t<0 indicating pFU-off. The y-axis gives the measured frequency of EEG activity. The black line shows the grand average of the 1050 Hz amplitude response for this condition, in SNR units of the baseline. Red indicates increase of brain activity at a given frequency over baseline (here in the gamma band) in terms of standard deviations above the mean; blue indicates decreased activity relative to baseline (here in the beta band) in terms of standard deviations above the mean. Shown are significant t-values for p<0.05, after a global cluster correction.